COMMUNICATION

Delivering anion transporters to lipid bilayers in water

Daniel A. McNaughton,[a] Tsz Ying (Teresa) To, [a,b] Bryson A. Hawkins,[c] David E. Hibbs,[c] and Philip A. Gale [a,d*]

Cyclodextrins have been employed as delivery agents for lipophilic anion transporters, which allow their incorporation into lipid bilayers without using an organic solvent or pre-incorporation.

The development of synthetic anion transporter systems to facilitate the transport of chloride or HCl across lipid bilayers[1] has been driven in recent years by the potential to discover new anti-cancer agents[2] and the development of 'channel replacement therapies'[3] to ameliorate the symptoms of diseases such as cystic fibrosis. Current approaches to delivering these anionophores to model lipid bilayer systems include pre-mixing the lipids with the transporter before vesicle formation (pre-incorporation)[4] or delivering the transporter to a suspension of vesicles in a small quantity of DMSO or other organic solvents.[5] Neither delivery method is ideal when studying the effect of anionophores on biological systems beyond cell cultures.

Cyclodextrins (CD) are a commercially available class of cyclic oligosaccharide[6] that have been used to encapsulate drug molecules to improve their water solubility and bioavailability.[7] We decided to employ this methodology to improve the deliverability of anionophores to lipid bilayer membranes. Adamantyl moieties form stable inclusion complexes with β-CD (typically K_a = 10^3–10^5 M^{-1}) due to their perfect size-fit complementarity with the hydrophobic cavity of β-CD.[8] Therefore, a novel series of adamantyl-appended transporters **1**–**6** (Fig. 1) were prepared with the intention that the formation of an inclusion complex with a β-CD derivative would enhance the aqueous solubility of the transporters, permitting their delivery to liposomal assays in pure water. Successful aqueous delivery would provide a proof of concept to support this method and allow these types of compounds to be studied in biological systems while avoiding potential toxicity from the use of an organic solvent.

Novel mono-(thio)urea compounds **1**, **2**, **3**, and **4** were prepared via condensation reactions between commercially available 1-adamantanemethylamine or 1-adamantylamine and the corresponding iso(thio)cyanate. Compounds **3** and **6** were readily obtained by reaction of either aminoadamantyl derivative with a 4-nitrophenyl squarate intermediate (see the ESI† for the experimental details, synthetic methods, and characterisation data). Single crystals of compound **1** suitable for X-ray diffraction were obtained in the presence of tetrabutylammonium chloride (TBACl) (20 equiv.) by slow evaporation of a saturated DMSO solution containing the two components. **1**·TBACl crystallised in the centrosymmetric triclinic $P\bar{1}$ space group (CDCC 2109213). The receptor was found to form a 1:1 receptor:anion complex with TBACl, shown in Fig 2, with coordinating hydrogen bonding interactions existing between chloride and the protons of the urea moiety (N···Cl distances: 3.145–3.278 Å, N–H···Cl angles: 150.5(7)–165.6(7)°). The crystal structures of compounds **1** and **3** are available in the ESI†.

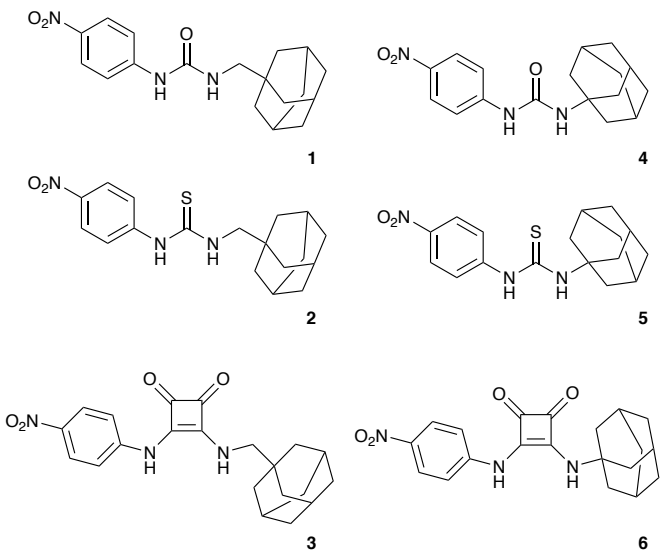

Figure 1 The structures of compounds **1** – **6**.

Proton NMR titrations were conducted for compounds **1**–**6** to assess their affinity for binding Cl^- (as TBACl) in DMSO-d_6/0.5% D_2O. The changes in the chemical shifts of the NH protons in each titration were followed and fit to a 1:1 host:guest binding model using the Bindfit applet.[9]

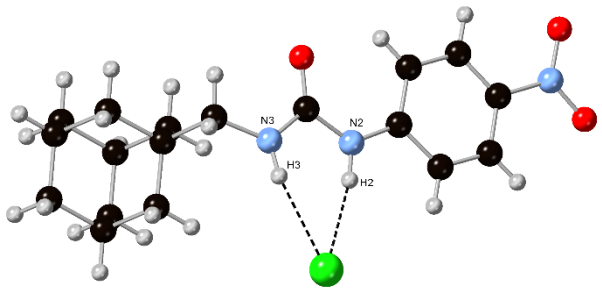

Figure 1 The single crystal X-ray structure of **1**·TBACl complex (CDCC 2109213). The tetrabutylammonium counter cation has been omitted for clarity.

As shown in Table 1, compounds **1**–**6** exhibit weak to moderate 1:1 binding to Cl^- in the competitive solvent media employed. The binding constants range from 21–249 M^{-1} and correlate with the acidity and potency of each species of hydrogen bond donor, and squaramide compounds **3** and **6** exhibits the series' highest binding affinity. Compounds **1**–**3**, which possess a methyl spacer incorporated between the hydrogen bond donor moiety and the adamantyl group, are stronger Cl^- binding receptors than compounds **4**–**6**. This difference in binding affinity suggests that the proximity of the adamantyl groups to the binding site could interfere with the approach of Cl^- during coordination and that binding is more efficient when the adamantyl group is permitted to orientate away from the binding site.

Table 1. Binding constants (K_a) for the complexation of compounds **1**–**6** and Cl^- (as the TBA salt) in DMSO-d_6/0.5% D_2O at 298 K

Compound	K_a(M^{-1}) [a,b]	Compound	K_a(M^{-1}) [a,b]
1	34	**4**	21
2	48	**5**	39
3	249	**6**	211

[a] All errors <6%. [b] Calculated with a 1:1 host:guest binding model using the online Bindfit applet.[9]

The chloride transport activity of compounds **1**–**6** was assessed using the Cl^-/NO_3^- exchange ISE assay. For these experiments, receptors were delivered to the experimental solution as an aliquot of DMSO solution. Large unilamellar vesicles (200 nm) were prepared with a NaCl internal solution (487 mM) buffered to pH 7.2 with sodium phosphate salts (5 mM). The vesicles were suspended in an external solution of $NaNO_3$ (487 mM), which was also buffered to pH 7.2 with sodium phosphate salts (5 mM) to give a lipid concentration of 1 mM. The experiments were initiated by adding a transporter as a DMSO aliquot (10 µL to a total volume of 5 mL) at t = 0 s, and chloride efflux was followed using a chloride ISE. Dose-response studies were performed across several concentrations of the transporter. Hill analysis was applied to obtain EC_{50} values (the concentration of transporter needed to achieve 50% chloride efflux after 270 s), Hill coefficients (which indicate the stoichiometry of the transport process), and initial transport rate at a 2 mol% loading of the transporter, with respect to concentration of lipid, which are shown in Table 2. In general, the trend in transporter activity reflects the trend in Cl^- binding affinity. Compound **3** was less active in the assay than expected, likely due to the poor solubility of this compound in aqueous solution. The thiourea and squaramide transporters exhibit reasonable levels of transport activity (EC_{50} = 0.31–0.47 mol%) and are comparable to other functionalised receptors that possess only a single hydrogen bond donor.[10]

Adamantyl groups have been appended to drug molecules to act as lipid solubilisers and enhance the ability of a compound to penetrate the blood-brain barrier.[11] The lipophilicities of compounds **1**–**6** was quantified using the online VCCLab ALOGPS2.1 applet,[12] and the values, shown in Table 2, ranged between 3.72–4.62. Despite the highly lipophilic character of the adamantane appendages, the log P values of the series fall within the range which is typically suitable to facilitate anion transport.[13] The Hill coefficients ranged from n = 1.6–2.7 and indicate a 2:1 transporter:chloride stoichiometry is required to facilitate transport. A 2:1 sandwich complex offers a greater degree of encapsulation around the chloride anion, shielding the charged species whilst traversing the non-polar interior of the bilayer. The initial transport rate calculated for **3** is the slowest of the series (k_{ini} = 0.5 % s^{-1}), despite the enhanced activity over the urea compounds **1** and **4** (k_{ini} = 1.7 and 1.0 % s^{-1}, respectively). This result again suggests that poor solubility impacts the rate of delivery of this transporter into the membrane.

Table 2. Summary of the anion transport parameters (EC_{50} and n), initial transport rates at a 2 mol% loading of the transporter (kini), and calculated lipophilicity values (clog P) for compounds **1**–**6.**

Compound	EC_{50} (mol%) [a]	Hill coefficient (n)	Initial transport rate (k_{ini}) (% s^{-1}) [b]	*c*log *P* [c]
1	0.80	2.4	1.7	4.22
2	0.37	2.4	11.0	4.62
3	0.47	1.8	0.5 [d]	3.90
4	0.95	2.1	1.0	3.99
5	0.45	1.6	3.8	4.45
6	0.31	2.7	3.1	3.72

[a] The EC_{50} at t = 270 s, shown as transporter:lipid molar percent. [b] Max initial transport rate (% s^{-1}) calculated at a transporter loading of 2 mol% by fitting an efflux plot to an exponential decay function. [c] Average *c* log *P* values calculated using VCCLab.[12] [d] Efflux plot fit to Boltzmann sigmoidal curve.

2-Hydroxypropyl-β-cyclodextrin (HP-β-CD), shown in Fig. 3, was employed as the host molecule due to its enhanced aqueous solubility relative to unsubstituted β-cyclodextrin. The formation of an inclusion complex with compounds **1**–**6** was attempted using a kneading method (method 1), and two methods involving microwave irradiation (methods 2 and 3), which differ in the amount of solvent used.[14] Each method involved using a 1:1 water:ethanol solvent mixture to ensure that both host and guest were partially solubilised, and each inclusion complex mixture was added to pure water after the completion of the inclusion process. The addition of water resulted in the precipitation of any uncomplexed transporter, which was filtered and removed, leaving a filtrate containing a mixture of free HP-β-CD host and the desired inclusion complex. A full description of the methods used to obtain the inclusion complexes can be found in the ESI†.

Evidence for the formation of an inclusion complex following each preparation method was initially assessed by obtaining a ^{1}H NMR spectrum of each inclusion complex mixture in D_2O. The presence of signals that can be reliably attributed to the guest transporter indicates that the molecule exhibits enhanced aqueous solubility due to the inclusion process. In the ^{1}H NMR spectra of HP-β-CD·**1** (methods 1–3), HP-β-CD·**2** (methods 1–3), HP-β-CD·**4** (methods 1–3), and HP-β-CD·**6** (methods 1–2), peaks attributed to the guest transporter are clearly visible and integrated to the expected ratio (shown in the ESI†).

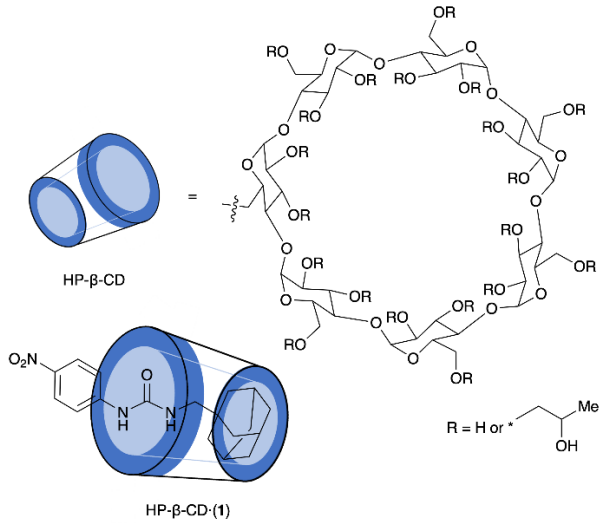

Figure 3 A schematic showing encapsulation of transporter **1** in HP-β-CD.

The inclusion complex was isolated as part of a mixture of free HP-β-CD and inclusion complex. The mass percentage of transporter present in each mixture was determined using UV-Vis studies in DMSO. Initially, UV-Vis spectra were collected at five concentrations (5–50 µM) for compounds **1**–**6**, calibration curves were constructed, and the molar extinction coefficient, ε, for each transporter was calculated. HP-β-CD is transparent in the tested UV-Vis region (Fig S96, ESI†), meaning any absorbances in the UV-Vis spectra of the inclusion complex mixtures were attributed solely to the transporter molecule. A mass for each inclusion complex mixture was recorded before a UV-Vis spectrum was obtained. The absorbance value, A, and the calculated ε in each case was used to determine the concentration of transporter present in the DMSO solutions and, therefore, the mass percentage of transporter relative to HP-β-CD in each mixture. Full details of the calculations and the mass percentages values for each inclusion mixture are reported in Section 9.2 of the ESI†.

Mass percentages of transporter present ranged from 1.8–6.9% (Table S10). The mixtures containing the highest mass percentage corresponded to approximately a 3:1 molar ratio of HP-β-CD to transporter. The microwave irradiation methods were generally more successful than kneading, which agrees with findings in the literature.[15] The inclusion of compound **3** was unsuccessful, which is likely due to the poor solubility of this receptor. The inclusion of compound **5** was similarly insufficient. The proximity of the adamantane to the bulky thiourea sulfur atom of this compound may sterically inhibit the approach of HP-β-CD. A mass percentage of >6% was calculated for compounds **6** (method 2) and **1**, **2,** and **4** (method 3), and these inclusion complex mixtures were investigated further.

Additional UV-Vis spectra were collected for HP-β-CD·**1**, HP-β-CD·**2**, HP-β-CD·**4** and HP-β-CD·**6**, dissolved in H_2O, and compared to the UV-Vis spectra of the free compounds in DMSO. An overlay of the UV-Vis traces of free transporter **1** dissolved in DMSO and the HP-β-CD·**1** complex dissolved in water can be viewed in Fig S97. The similarity in the absorbance profile at similar wavelengths of 342 nm (H_2O) and 354 nm (DMSO) suggested that compound **1** is present in the inclusion mixture dissolved in H_2O and that an inclusion complex has been prepared successfully. Overlaid spectra of the other inclusion complexes are shown in the ESI† (Fig S97–S100).

FTIR spectra of the four inclusion complex mixtures and the free compounds were obtained, and the characteristic stretches were compared. A decrease in intensity, a shift in wavenumber, or the disappearance of stretches associated with the guest can all support the formation of an inclusion complex due to restriction of the guest stretching vibrations when included within the HP-β-CD cavity.[16] However, the high mass content of HP-β-CD present means bands associated with this component are more intense, leading to overlap and obscuring of bands associated with the guest molecules.[17] Nevertheless, distinct differences were observed upon a comparison of the spectra, described in the ESI†.

The 2D NOESY ^{1}H NMR spectra collected for the four mixtures (Fig S118-S129) provided the strongest evidence for the formation of inclusion complexes. NOE cross-peaks can be clearly seen between the resonances attributed to the guest adamantyl protons and the protons which line the internal cavity of HP-β-CD. This proximity suggests that an inclusion complex has formed between the two components and is complemented by the absence of cross-peak correlations associated with other HP-β-CD protons located on the outer surface of the structure. Interestingly, cross-peak interactions were also visible between the internal HP-β-CD protons and the signals related to the aryl protons of the guest molecules. One explanation for these findings is that the adamantane sits in the primary rim of HP-β-CD whilst the remainder of the molecule penetrates the cavity. Another possibility is that both end groups are included inside a CD molecule, forming a 2:1 host:guest complex. Both configurations would minimise the exposure of the aromatic unit to surrounding water molecules, which otherwise would inhibit aqueous solubility.

The transport capabilities of the inclusion complexes were investigated using the Cl^-/NO_3^- exchange ISE assay. The conditions employed were near-identical to those employed for studies on the free transporter; however, the HP-β-CD·transporter complexes were delivered in an aliquot of pure water. The transporter mass percentage values calculated previously were applied to provide the mass of the inclusion complex required to give a certain concentration of transporter (mol%) in aqueous solution. A control run with only HP-β-CD present resulted in no Cl^- efflux. The transport parameters calculated for each complex are shown in Table 3.

Encouragingly, the results indicated that the transporters could be successfully delivered to the vesicles and that delivery as an inclusion complex facilitated Cl^- transport with minimal depreciation in activity. The dose response efflux plots for **1** when delivered in DMSO are very similar to the efflux plots for inclusion complex HP-β-CD·**1** when delivered in H_2O, which are both shown in Fig. 4. The EC_{50} values of the inclusion complexes all differ by less than 30% of the DMSO-delivered transporters in Table 2. Comparable levels of activity are gratifying but perhaps surprising result. To cross the membrane, the transporter molecule must first decomplex from the CD host. These findings show that this process does not hamper deliverability into the lipid bilayer.

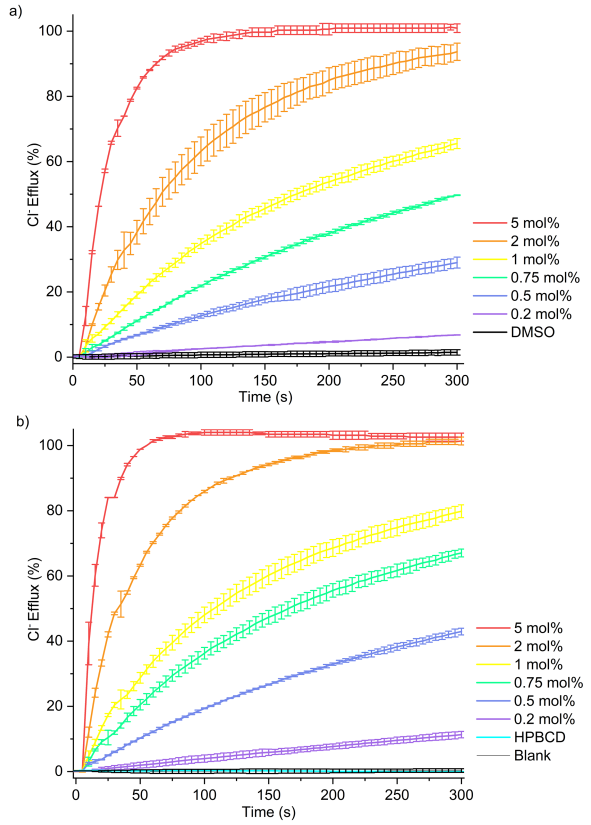

Figure 4 Dose-response studies for compound **1** using the Cl^-/NO_3^- ISE assay. a) Delivered as a free transporter in DMSO solution. b) Delivered as an inclusion complex HP-β-CD·**1** in water. Each data point is the average of two repeats with error bars to show standard deviation.

In summary, a series of adamantyl-functionalised transporters were synthesised and included inside the cavity of HP-β-CD to improve their aqueous deliverability. Following confirmation of the formation of inclusion complexes, liposomal chloride transport studies found that the complexes did not limit transport activity compared with delivery of the anionophores in DMSO. These findings highlight the potential for cyclodextrin inclusion complexes to be employed as delivery vehicles to examine the properties of anion transporters *in vitro* and *in vivo* in the absence of DMSO. Deliverability and activity in purely aqueous environments are key steps towards anion transporters finding future real-world applications.

DAM, TYT, BH, DEH and PAG acknowledge and pay respect to the Gadigal people of the Eora Nation, the traditional owners of the land on which we research, teach, and collaborate at the University of Sydney. PAG thanks the Australian Research Council (DP200100453) and the University of Sydney for funding.

Table 3 Summary of the anion transport parameters (EC_{50} and n) and initial transport rates at a 2 mol% loading of the transporter (k_{ini}) for the HP-β-CD·transporter inclusion complexes, delivered to vesicles as solutions of pure water

Compound	EC_{50} (mol%) [a]	Hill Coefficient (n)	Initial Transport Rate (k_{ini}) (% s^{-1}) [b]
HP-β-CD·1	0.62	3.3	4.8
HP-β-CD·2	0.38	1.2	23.6
HP-β-CD·4	1.22	1.9	0.6
HP-β-CD·6	0.39	1.9	2.2

[a] The EC_{50} at t = 270 s, shown as transporter:lipid molar percent. [b] Max initial transport rate (% s^{-1}) calculated at a transporter loading of 2 mol% by fitting an efflux plot to an exponential decay function.

Conflicts of Interest

There are no conflicts of interest to declare.

Notes and references

1 J.T. Davis, P.A. Gale and R. Quesada, *Chem. Soc. Rev.,* 2020, **49**, 6056-6086.
2 (a) S.-H. Park, S.-H. Park, E.N.W. Howe, J.Y. Hyun, L.-J. Chen, I. Huang, G. Vargas-Zuñiga, N. Busschaert, P.A. Gale, J.L. Sessler, I. Shin, *Chem*, 2019, **5**, 2079-2098; (b) N. Busschaert, S.-H. Park, K.-H. Baek, Y.P. Choi, J. Park, E.N.W. Howe, J.R. Hiscock, L.E. Karagiannidis, I. Marques, V. Félix, W. Namkung, J.L. Sessler, P.A. Gale and I. Shin, *Nature Chem.*, 2017, **9**, 667-675.
3 H. Li, H. Valkenier, A.G. Thorne, C.M. Dias, J.A. Cooper, M. Kieffer, N. Busschaert, P.A. Gale, D.N. Sheppard and A.P. Davis, *Chem. Sci.* 2019, **10**, 9663-9672.
4 J.A. Cooper, S. T. G. Street, A. P. Davis, *Angew. Chem. Int. Ed.*, 2014, **53**, 5609-5613.
5 L.A. Jowett and P.A. Gale, *Supramol. Chem.*, 2019, **31**, 297-312.
6 (a) J. Szejtli, *Chem. Rev.*, 1998, **98**, 1743-1754; (b) G. Crini, *Chem. Rev.*, 2014, **114**, 10940-10975.
7 A. Haimhoffer, Á. Rusznyák, K. Réti-Nagy, G. Vasvári, J. Váradi, M. Vecsernyés, I. Bácskay, P. Fehér, Z. Ujhelyi and F. Fenyvesi, *Sci. Pharm.*, 2019, **87**, 33.
8 R. Palepu and V. C. Reinsborough, *Aust. J. Chem.*, 1990, **43**, 2119-2123.
9 D. B. Hibbert and P. Thordarson, *Chem. Commun.,* 2016, **52**, 12792-12805.
10 (a) S. N. Berry, V. Soto-Cerrato, E. N. W. Howe, H. J. Clarke, I. Mistry, A. Tavassoli, Y.-T. Chang, R. Pérez-Tomás and P. A. Gale, *Chem. Sci.*, 2016, **7**, 5069-5077; (b) X. Bao, X. Wu, S. N. Berry, E. N. W. Howe, Y.-T. Chang and P. A. Gale, *Chem. Commun.*, 2018, **54**, 1363-1366.
11 (a) J. M. Scherrmann, Vascul. Pharmacol., 2002, 38, 349-354; (b) N. Tsuzuki, T. Hama, M. Kawada, A. Hasui, R. Konishi, S. Shiwa, Y. Ochi, S. Futaki and K. Kitagawa, J. Pharm. Sci., 1994, 83, 481-484; (c) M. A. Ilies, B. Masereel, S. Rolin, A.

Scozzafava, G. Câmpeanu, V. Cîmpeanu and C. T. Supuran, Biorg. Med. Chem., 2004, 12, 2717-2726.
12 (a) I. V.Tetko and V. Y.Tanchuk, ALOGPS 2.1 (http://www.vcclab.org) is a free on-line Program to Predict logP and logS of Chemical Compounds; (b) I. V. Tetko and V. Y. Tanchuk , *J. Chem. Inf. Comput. Sci.*, 2002, **42** , 1136 — 1145.
13 (a) V. Saggiomo, S. Otto , I. Marques , V. Félix , T. Torroba and R. Quesada , *Chem. Commun.*, 2012, **48** , 5274 —5276; (b) N. Busschaert, S.J. Bradberry, M. Wenzel, C.J.E. Haynes, J.R. Hiscock, I.L. Kirby, L.E. Karagiannidis, S.J. Moore, N.J. Wells, J. Herniman, G.J. Langley, P.N. Horton, M.E. Light, I. Marques, P.J. Costa, V. Félix, J.G. Frey and P.A. Gale, Chem. Sci., 2013, **4**, 3036-3045; (c) H. Valkenier, C.J.E. Haynes, J. Herniman, P.A. Gale and A.P. Davis, Chem. Sci. 2014, **5**, 1128-1134 (d) M. J. Spooner and P. A. Gale , *Chem. Commun.*, 2015, **51** , 4883 —4886; (e) N.J. Knight, E. Hernando, C.J.E. Haynes, N. Busschaert, H.J. Clarke, K. Takimoto, M. García-Valverde, J.G. Frey, R. Quesada and P.A. Gale, Chem. Sci., 2016, **7**, 1600-1608.
14 (a) K. P. Sambasevam, S. Mohamad, N. M. Sarih and N. A. Ismail, *Int. J. Mol. Sci.*, 2013, **14**, 3671-3682; (b) S. Riela, G. Lazzara, P. Lo Meo, S. Guernelli, F. D'Anna, S. Milioto and R. Noto, *Supramol. Chem.*, 2011, **23**, 819-828.
15 (a) A. Figueiras, L. Ribeiro, M. T. Vieira and F. Veiga, *J. Incl. Phenom. Macrocycl. Chem.*, 2007, **57**, 173-177; (b) S. Prabu, M. Swaminathan, K. Sivakumar and R. Rajamohan, *J. Mol. Struct.*, 2015, **1099**, 616-624.
16 P. Mura, *J. Pharm. Biomed. Anal.*, 2015, **113**, 226-238.
17 O. Adeoye, C. Costa, T. Casimiro, A. Aguiar-Ricardo and H. Cabral-Marques, *J. Supercrit. Fluids*, 2018, **133**, 479-485.